ADMINISTRATIEVE GEGEVENS & TECHNISCHE GEGEVENS

Kaart nr.:	115E
PLAAT:	ITTRE
Nr.:	**0912 (VIII, c)**
Type Boring:	**ontsluiting N.A.S. 2**
Topografische kaart:	**39/2**
Uitgevoerd te:	Ittre
Postnr.:	1460
Adres boorplaats:	Along the Brussel-Charleroi canal, between 40590 m and 41110 m (distance along E-side canal, from Charleroi to Brussels)
Opdrachtgever:	
Boorfirma:	
Boordatum/terreinopname:	September 2001
Topografie:	BGD, topo 1/10000
Stalen door:	
Boormethode:	ontsluiting
Lengte & doormeters:	
Grondwaterstanden:	
1ste maal:	
Bij rust:	
Tijdens pompen:	
Debiet:	
Waterzaaknr.:	
Totale diepte:	
Stalen bewaard:	staalname en bewaring door auteur
Maaiveld / ref. peil:	+- 80 m
X:	140750 (center)(min 140660 – max 140850)
Y:	148470 (center)(min 148240 – max 148660)
NIS code:	25044

LITHOLOGISCHE BESCHRIJVING

Short description of outcrop Northern Asquempont section 2 (BGD115E0912), its immediate surroundings and its importance (fig. 1)

In the Lembeek area, in the southern part of the Cambrian core of the Brabant Massif, several researchers observed steeply plunging folds (Vander Auwera, 1983; Verniers, unpub. data 1993, André, pers. comm. 2000). Although their orientation markedly differs from the folds in the Ordovican-Silurian formations in the southern part of the massif, Sintubin *et al.* (1998) demonstrated that also these folds formed cogenetically with cleavage development. Largely based on aeromagnetic data, Sintubin *et al.* (1998) attributed the apparent division in fold style between the Cambrian on the one hand and the Ordovician-Silurian on the other hand, to dextral transpression along the Asquempont lineament, wrongly attributed to the Asquempont fault. However, the observations of Debacker (2001) and Debacker *et al.* (2003, 2004a) put strong doubt on the role of the Asquempont fault in dividing both fold types. Firstly, the Asquempont fault (F8) does not coincide with the pronounced NW-SE-trending aeromagnetic Asquempont lineament. Secondly, if the Asquempont fault (F8) pre-dates cleavage development and folding, it would seem highly unlikely that F8 would be responsible for a division between the two fold styles, both of which are considered cogenetic with cleavage development. Thirdly, there is evidence for sub-horizontal to moderately plunging folds north of F8. Small changes in bedding dip and the orientation of the cleavage/bedding intersection in the Cambrian part of outcrops central Asquempont section 2 and Virginal railway section 1 suggest sub-horizontal to moderately plunging folds. In addition, at the N-end of outcrop central Asquempont section 2, a moderately NW-plunging antiformal step fold occurs (see above) and also Herbosch (pers. comm. 2000) observed a synformal step fold in the eastern part of the outcrops of “Rue de l’ancien canal” (location: see 128E0753, fig. 2).
As such, it appears that, if outcropping, the transition between both fold types should be sought north of the Asquempont fault, between the Asquempont area to the south and the Lembeek-Clabecq area to

the north. This area comprises two lithological units. The upper unit consists of greenish grey, soft, porous mudstones of the Asquempont Member, Oisquercq Formation. The lower unit, also belonging to the Oisquercq Formation, consists of dark purplish grey to blue claystones and mudstones of the Ripain Member. Although also the Ripain Member contains zones of greenish grey mudstone, these generally differ from the Asquempont Member by their hardness and low porosity (cf. Verniers *et al.*, 2001). Unfortunately, both members are characterised by an extreme homogeneity. To the author's knowledge, prior to this study only a few bedding planes were ever observed in the Oisquercq Formation in the Asquempont area (outcrop northern Asquempont section 3, Legros, 1991; cf. Lenoir, 1987).
Outcrop northern Asquempont section 2 (N.A.S. 2; BGD115E0912) contains the transition between the Asquempont Member and the Ripain Member, as well as a transition zone between steeply plunging (cf. Sintubin *et al.*, 1998) and gently plunging folds, both being cogenetic to the same cleavage (fig. 2 & 3). The results of the data of northern Asquempont section 2, derived from Debacker (2001) and presented herein, were published by Debacker *et al.* (2004b). In addition, because of the variable fold orientations, and the extreme homogeneity of both members along outcrop northern Asquempont section 2, this outcrop was used also for detailed magnetic fabric analyses, of which the results can be found in Debacker *et al.* (2004c, 2005). Below, the observations of Debacker (2001) are given. In the (rare) cases in which extra information is given resulting from observations from the period 2001-2005, this is mentioned specifically.

1. Macroscopic observations

Cleavage/fold relationship

Cleavage, bedding and fracture data are shown in tables 1, 3 and 4. The transition between the Asquempont Member and the Ripain Member, approximately 10 m wide, was found at the western end of outcrop Ittre 1, the northern end of outcrop northern Asquempont section 2 (N.A.S. 2, ~41020 m, cf. Legros, 1991; Hennebert & Eggermont, 2002) and its position could be deduced between 2 outcrops in the abandoned railway at Virginal (between 7965 m and 7830 m). Within N.A.S. 2, the outcrop trace of this transition suggests a relatively high strike and a steeply dipping to sub-vertical bedding. New observations (period 2001-2005) indicate that, despite of the apparent width of the transition between both members in terms of distance along the outcrop (seemingly ~10 m), the actual transition between both members is only 1 to 2 metres wide. The apparently large width is entirely due to the relative orientation of bedding, being subvertical, with a trend at very low angles to the trend of the outcrop. As both members have different magnetic properties, magnetic fabric analyses allow pinpointing this transition much better than standard lithological observations do (Debacker *et al.*, 2004c, 2005). On the basis of the magnetic properties, sample TD1010 is considered to be situated at or very close to the transition between both members (see table 2 for location).
Along the Brussel-Charleroi canal, a gradual change in cleavage dip can be observed. Going from south to north, cleavage dip changes from 50°NE in outcrop N.A.S. 1 and the southern parts of outcrops N.A.S. 2 and 3, towards 80°NE in outcrop N.A.S. 4 and the northern parts of outcrop N.A.S. 2. Further north, in outcrops Oisquercq 1 to Oisquercq 4, cleavage remains steeply NE-dipping (approximately 80°NE). Apart from outcrop Ittre 3, bedding is only observed in outcrops N.A.S. 2 and 3 and locally in outcrop Oisquercq 1.
Within outcrop N.A.S. 2 (table 3) bedding is frequently observed in outcrop and where field observations do not allow determining bedding, cut oriented hand specimens often do. In outcrop, bedding is locally revealed by sedimentary ripples and a thin volcanic intercalation, usually by less obvious features such as cleavage refraction, vague changes in grain size and/or colour on fresh fracture surfaces. Only occasionally do cut oriented hand specimens give away bedding directly by a change in grain size. Usually, however, the darker colour of the grey clayey bands in the greenish grey homogeneous mudstone is much easier to use. Often bedding can only be determined in outcrop after linking planar surfaces with bedding determined on nearby situated cut hand specimens.
As appears from bedding measurements and the orientation of the cleavage/bedding intersection, sub-horizontal to gently plunging fold hinges lines and associated intersection lineation take up a large part of the section and dominate the southern part of the outcrop. The folds have gentle to open interlimb angles, are asymmetric, with a SW-verging asymmetry and a step fold-like geometry. Because of their analogy with the fold orientations in the Ordovician and Silurian, the gently plunging folds are labelled

type A folds (see Debacker, 2001). In between these zones of type A folds, zones with a moderately to locally steeply NE-, E-, to SE-plunging cleavage/bedding intersection occur. Especially in the northern part of the outcrop the intersection lineation is steeply plunging and clearly differs from the cleavage/bedding intersection associated with the type A folds. Also the bedding measurements suggest moderately to steeply SE-plunging folds. Unfortunately, however, individual fold hinges were not observed. This is probably due to a combination of the relative orientation of the outcrop, the homogeneity of the deposits, and the unfamiliarity with such bedding and fold orientations. Bedding in the Ripain Member, in the northern part of the outcrop, where a steep intersection lineation predominates, is even more difficult to observe than in the Asquempont Member. In these rocks, bedding is often reflected by small chloritic bands. Although Legros (1991) argued that these have a tectonic origin, parallelism between one of these bands and a nearby plane containing sedimentary ripples suggests a parallelism to bedding of at least some of the chloritic bands. A further complication is the apparent predominance of steeply NE-dipping bedding, resulting in a shortage of bedding measurements at high angles to cleavage, necessary to constrain the fold hinge line attitude. If the bedding poles indicative of a position in the fold hinge zones are not taken into account, the resulting fold hinge line could have a moderate to gentle plunge, and one might tend to attribute the steep to moderate intersection as a result of the low angle between bedding and cleavage (~ 20°). However, stereographic manipulations, taking into account the measured angles between cleavage and bedding and allowing for an angle of transection up to 020° show that the cleavage/bedding intersection indeed reflects moderately to steeply plunging folds. For matters of convenience these folds will be termed type B folds.
On the basis of the orientation of bedding, cleavage/bedding intersection and fold hinge lines outcrop N.A.S. 2 can be divided into four large parts (> 50 m wide), two containing type A folds, and two of which the data suggest type B folds. In between, smaller zones may be distinguished (e.g. between 40825 m and 40850 m). As becomes apparent from table 3, also the cleavage orientation seems to change with fold type. The two large zones with moderately to steeply plunging fold hinge lines and intersection lineation have slightly higher strike values than the two zones with type A folds. This change in cleavage trend does not reflect the small intermediate zones. A pronounced anticlockwise axial cleavage transection dominates this outcrop, apparently irrespective of fold type.

Fractures

In outcrops N.A.S. 2 steep fractures oriented at high angles to the structural trend often contain a thin quartz infill, with an alignment parallel to the cleavage/fracture intersection. Although, throughout the outcrop, the trend of the fractures remains fairly constant, a change in dip occurs. In the zones with type A folds, fractures are sub-vertical to steeply E-dipping, whereas, in the zones where a moderately to steeply E-plunging cleavage/bedding intersection occurs, the fractures are steeply to moderately W-dipping (tables 1 & 4).

Faults and slip planes

Outcrop N.A.S. 2 contains several relatively wide zones of fracturation, post-dating cleavage development. Their outcrop trace usually suggests a steep NW- to NNW-trending orientation. The central parts of these fracturation zones often contain fine crush breccias. Several of these zones occur around the transition between the zones with different fold styles (e.g. around 40830 m and between 40860 and 40870 m). At 40903 m, a 1 m-wide steeply S-dipping contractional kink band occurs, with a down-throw towards the south, and a small normal fault running along the kink band boundary. Although no striations are observed, the geometry of the overall structure suggests a predominantly dip-slip displacement.
Many planar surfaces contain lineations resembling striations. Often, however, these can be shown to represent an intersection lineation (e.g. intersection with cleavage). Only those lineations/striations of which the orientation clearly deviates from an intersection lineation are considered. In several places steeply NW-plunging striations occur on sub-vertical to moderately dipping bedding planes, with an apparent down-throw towards the SE. Locally, sub-horizontal to gently NW-plunging striations occur on bedding planes, with an unknown sense of movement (e.g. at 40835 m), as well as moderately E-plunging striations on sub-vertical E-W-trending fractures (e.g. at 40974 m). In the northern part of the outcrop several gently SE-plunging striations occur, with an apparently dextral sense of movement, on

sub-vertical planes with an orientation parallel to bedding.

2. Microscopic observations

Thin sections

Bedding in the Oisquercq Formation is even more difficult to observe in thin section than on cut hand specimens. Only in two samples bedding was recognised on a microscopic scale. In both samples (TD181, Asquempont Member and TD256, Ripain Member) bedding becomes apparent by means of a gradual change in colour, related to an increase in amount of opaque material. Although macroscopically changes in grain size have been observed in the Oisquercq Formation (e.g. TD123 in outcrop Virginal railway section 1) the faint change in colour in these two samples is not associated with a recognisable change in grain size. On a microscopic scale, the only lithological difference observed between the Asquempont Member and the Ripain Member is the slightly higher amount of opaque material in the latter member.
Both lithologies are very fine-grained: detrital quartz grains are rarely observed. Only locally, quartz grains up to 25 microns are visible. A large amount of white mica is present, oriented parallel to the cleavage. The cleavage, however, is poorly pronounced. In contrast to the cleavage in the other studied lithologies (e.g. Rigenée Formation, Ittre Formation), usually of a disjunctive nature, with clear pressure solution seams, there is no clear observation of a spaced cleavage in the rocks of the Oisquercq Formation. Well-developed cleavage domains, marked by a, probably pressure solution-related, higher concentration of opaque material, appear to be absent and white mica seems to occur throughout the rock mass. Only occasionally do extremely vague cleavage-parallel anastomosing alignments of darker material, resembling cleavage domains, become apparent. Where observed, the estimated spacing of these is highly variable. In general, these cleavage domains are better developed in the Ripain Member than in the Asquempont Member. Also the alignment of white mica is more pronounced in the Ripain Member. This is compatible with the macroscopic cleavage appearance, being more widely spaced and much less pronounced in the Asquempont Member and having a better developed, slaty appearance in the Ripain Member.
As such, it seems that the cleavage in the Oisquercq Formation is a continuous to poorly developed anastomosing spaced cleavage, the continuous nature reflected by white mica, the spaced nature by vague cleavage domains with a gradual transition towards the microlithons. A spaced cleavage becomes apparent around the chlorite-mica stacks. As in the other investigated lithologies, also here stacks oriented parallel to cleavage as well as stacks oriented parallel to bedding occur. The latter, having lower aspect ratios than the former, are often flanked by pressure solution seams. Their orientation with respect to cleavage suggests a disjunctive cleavage nature.
We suggest that, on the scale of observation, the continuous to poorly developed disjunctive nature of the cleavage is mainly a result of the fine-grained extremely homogeneous nature of these deposits. Probably a strain partitioning occurs on a scale too small to be recognised by means of an optical microscope. To a large extent this is confirmed by the pole figure goniometry results.

Pole figure goniometry

X-ray pole figure goniometry was performed by M. Sintubin at Katholieke Universiteit Leuven. For information regarding the acquisition and interpretation of X-ray pole figure goniometry data, the reader is referred to Sintubin (1994).
Three types of pole figure patterns can be distinguished. The first type is observed around the transition zone between the Asquempont Member and the Ripain Member and in the Ripain Member (samples TD279 and TD256). This type is characterised by a moderate preferred orientation for both white mica and chlorite. The maxima coincide with the centre of the pole figure, which represents the cleavage pole. The pole figure pattern essentially reflects a flattening fabric. In the case of sample TD256 the pole figure pattern has a slightly orthorhombic symmetry, with a steeply plunging short axis. This short axis may correspond to an intersection lineation between cleavage and bedding, which is compatible with the macroscopically observed steeply plunging cleavage/bedding intersection. The small differences between the relative amount of preferred orientation of chlorite and white mica in the one sample with respect to the other sample, and the small difference in pole figure pattern may be a result of lithology.

****

The second type, obtained from two samples of the Asquempont Member (TD186 and TD197), has a weak to moderate preferred orientation, with rather orthorhombic pole figure patterns. The pole figure maxima of white mica and chlorite approximately coincide. In the case of sample TD186, the degree of preferred orientation of white mica is similar to that of chlorite, whereas in sample TD197, chlorite shows a stronger preferred orientation than white mica. In both cases, the short axis of the orientation distribution is steeply plunging. However, whereas in sample TD186, this is reflected by mica and, to a lesser extent, by chlorite, this pattern is only reflected by the chlorite orientation distribution in sample TD197. As macroscopically observed, the former sample has a moderate to steep cleavage/bedding intersection, whereas the latter has a gently plunging intersection lineation. As suggested by Sintubin (pers. comm. 2001) this second type of pole figure pattern possibly results from a small angle between bedding and cleavage. The macroscopic data point to an angle between cleavage and bedding of 40° in sample TD197 and 23 to 33° in sample TD186.
The third type differs from the other two types by its clear girdle pole figure pattern, a relatively weak degree of preferred orientation, which is always higher for chlorite than for white mica and different pole figure maxima for chlorite and for mica. The girdle pattern is generally more pronounced for mica than for chlorite. All samples (TD185, TD272, TD192, TD276, TD195, TD196 and TD248) are taken from the Asquempont Member. The girdle pattern and the different pole figure maxima of chlorite and mica point to an intersection pole figure (cf. Sintubin, pers. comm. 2001). Compatible with the optical observations, the mica pole figure maxima coincide with the cleavage pole, generally occupying a central position within the pole figures. Therefore, probably the chlorite pole figure maxima coincide with the bedding poles. This is confirmed by a comparison with the macroscopically determined angles between bedding and cleavage (table 3). Large differences between chlorite and mica pole figure maxima are obtained from samples in which the angle between bedding and cleavage varies between 74 and 79° (TD192, TD195, TD196). Those with moderate angles between both pole figure maxima are obtained from samples TD276 and TD248, having cleavage/bedding angles of respectively 39 and 61°. Small to moderate angles are suggested for sample TD185, having a cleavage/bedding angle of 50°. A small angle between the chlorite and mica pole figure maxima is obtained for sample TD272, having an angle between cleavage and bedding of only 17°. As such, these pole figure patterns seem strongly influenced by the angle between cleavage and bedding. The short axes of the girdle should correspond to the cleavage/bedding intersection lineation. Also this corresponds to the macroscopic observations. Although, mainly because of small irregularities during sample preparation (e.g. a slightly oblique cutting), care should be taken in using the apparent plunge values of the orientation distribution short axes, these plunges generally match the plunge of the macroscopically determined cleavage/bedding intersection lineation. Pole figure patterns of samples from zones with sub-horizontal to gently plunging fold hinge lines and associated cleavage/bedding intersection have sub-horizontal orientation distribution short axes (samples TD185, TD195, TD196), whereas those from zones with moderately to steeply plunging folds (TD272, TD192) have plunging orientation distribution short axes. In two samples (TD276, TD248) a difference is observed, the short axis having a slightly higher plunge than that of the cleavage/bedding intersection determined in outcrop. Possibly this is due to irregularities during sample preparation.
As such, the pole figure data largely confirm the presence of zones with a moderately to steeply plunging intersection lineation in between zones with a sub-horizontal to gently plunging intersection lineation. The degree of alignment is compatible with a poorly to moderately developed cleavage, in general governed by white mica, acting on a bedding-parallel fabric usually reflected by chlorite. Although thin sections often suggest a poorly developed continuous cleavage, the pole figure goniometry data confirm our suggestion of a bimodal cleavage nature, with a crenulation or disjunctive fabric on a sub-microscopic scale. Depending on lithology and relative orientation of bedding and cleavage, the pole figure patterns may vary significantly.

References

DEBACKER, T.N. 2001. *Palaeozoic deformation of the Brabant Massif within eastern Avalonia: how, when and why?* Unpublished Ph.D. thesis, Laboratorium voor Paleontologie, Universiteit Gent.
DEBACKER, T. N., HERBOSCH, A., SINTUBIN, M., VERNIERS, J. 2003. Palaeozoic deformation history of the Asquempont-Virginal area (Brabant Massif, Belgium): large-scale slumping, low-angle

****

extentional detachment development (the Asquempont fault redefined) and normal faulting (the Nieuwpoort-Asquempont fault zone). *Memoirs of the Geological Survey of Belgium*, **49**, 1-30.
DEBACKER, T. N., HERBOSCH, A., VERNIERS, J., SINTUBIN, M. 2004a. Faults in the Asquempont area, southern Brabant Massif, Belgium. *Netherlands Journal of Geosciences/Geologie en Mijnbouw*, **83**, 49-65.
DEBACKER, T. N., SINTUBIN, M., VERNIERS, J. 2004b. Transitional geometries between gently plunging and steeply plunging folds: an example from the Lower Palaeozoic Brabant Massif, Anglo-Brabant deformation belt, Belgium. *Journal of the Geological Society, London*, **161**, 641-652.
DEBACKER, T. N., ROBION, P., SINTUBIN, M. 2004c. The anisotropy of magnetic susceptibility (AMS) in low-grade, cleaved pelitic rocks: influence of cleavage/bedding angle and type and relative orientation of magnetic carriers. In: Martin-Hernandez, F., Lüneburg, C.M., Aubourg, C. & Jackson, M. (eds.) *Magnetic Fabrics: Methods and Applications*. Geological Society, London, Special Publications, **238**, 77-107.
DEBACKER, T. N., ROBION, P., SINTUBIN, M. 2005. Complexity of the anisotropy of magnetic susceptibility in single-phase deformed, low-grade, cleaved Mudstone. *Materials Science Forum*.
HENNEBERT, M. & EGGERMONT, B. 2002. Carte Braine-le-Comte - Feluy n° 39/5-6, Carte géologique de Wallonie, échelle 1/25000. Namur: Ministère de la Région Wallonne.
LEGROS, B. 1991. *Etude structurale du Cambro-Ordovicien de la vallée de la Sennette (Massif du Brabant) – Belgique*. Unpublished M.Sc.-thesis, Université Catholique de Louvain.
LENOIR, J. L. 1987. *Etude cartographique, pétrographique et palynologique de l'Ordovicien inférieur du bassin de la Senne.* Unpublished M.Sc. thesis Université Libre de Bruxelles.
SINTUBIN, M. 1994. Textures in shales and slates. In: Bunge, H. J., Siegensmund, S., Skrotski, W. & Weber, K. (eds.) *Textures of Geological Materials.* DGM Informationsgesellschaft, Verlag, 221-229.
SINTUBIN, M., BRODKOM, F., LADURON, D. 1998. Cleavage-fold relationships in the Lower Cambrian Tubize Group, southeast Anglo-Brabant Fold Belt (Lembeek, Belgium). *Geological Magazine*, **135**, 217-226.
VANDER AUWERA, J. 1983. *Étude pétrographique, sédimentologique et géochimique de l'Assise de Tubize (DV2) - Massif du Brabant - Belgique*. Unpublished M.Sc. thesis, Université Libre de Bruxelles.
VERNIERS, J., HERBOSCH, A., VANGUESTAINE, M., GEUKENS, F., DELCAMBRE, B. PINGOT, J.L., BELANGER, I., HENNEBERT, DEBACKER, T., SINTUBIN, M. & DE VOS, W. 2001. Cambrian-Ordovician-Silurian lithostratigraphical units (Belgium). *Geologica Belgica*, **4**, 5-38

Timothy N. Debacker
September 2001

STRATIGRAFISCHE INTERPRETATIE

Oisquercq Formation, Asquempont Member to the south and Ripain Member to the north, based on Hennebert & Eggermont (2002) and Verniers *et al.* (2001). The transition occurs around ~41020 m in a seemingly ~10 m wide zone. However, the actual transition is only 1 to 2 m wide, the large apparent width in outcrop (~10 m) being due to the steep bedding dip and the small difference in trend between bedding and outcrop.

AUTEUR Debacker T.N., September 2001, with some added observations from period 2001-2005

Relevant documents for additional reading :

DEBACKER, T.N. 2001. *Palaeozoic deformation of the Brabant Massif within eastern Avalonia: how, when and why?* Unpublished Ph.D. thesis, Laboratorium voor Paleontologie, Universiteit Gent.

DEBACKER, T. N., ROBION, P., SINTUBIN, M. 2004. The anisotropy of magnetic susceptibility (AMS) in low-grade, cleaved pelitic rocks: influence of cleavage/bedding angle and type and relative orientation of magnetic carriers. In: Martin-Hernandez, F., Lüneburg, C.M., Aubourg, C. & Jackson, M. (eds.) *Magnetic Fabrics: Methods and Applications*. Geological Society, London, Special Publications, **238**, 77-107.

****

DEBACKER, T. N., SINTUBIN, M., VERNIERS, J. 2004. Transitional geometries between gently plunging and steeply plunging folds: an example from the Lower Palaeozoic Brabant Massif, Anglo-Brabant deformation belt, Belgium. *Journal of the Geological Society, London*, **161**, 641-652.

VERNIERS, J., HERBOSCH, A., VANGUESTAINE, M., GEUKENS, F., DELCAMBRE, B. PINGOT, J.L., BELANGER, I., HENNEBERT, DEBACKER, T., SINTUBIN, M. & DE VOS, W. 2001. Cambrian-Ordovician-Silurian lithostratigraphical units (Belgium). *Geologica Belgica*, **4**, 5-38.

BIJLAGEN

Table 1: Orientation data of structural elements in outcrop northern Asquempont section 2 (BGD115E0912).

Large 520 m-long outcrop situated along the E-side of the Brussel-Charleroi canal, just north of the Asquempont bridge, between 40.590 and 41.110 km. The transition between the Asquempont Member (SW) and the Ripain Member (NE) occurs in a seemingly ~10 m wide zone around 41.020 km (cf. Hennebert & Eggermont, 2002). However, new observations (period 2001-2005) indicate that, despite of the apparent width of the transition between both members in terms of distance along the outcrop, the actual transition between both members is only 1 to 2 metres wide. The apparent 10 m-width is entirely due to the relative orientation of bedding, being subvertical, with a trend at very low angles to the trend of the outcrop. Sample TD1010 is considered situated at or very close to the transition (see table 2). The importance of this outcrop is that it not only shows bedding in the Oisquercq Formation (locally even with sedimentary ripples and a small volcanic intercalation), but also suggests the presence of two different fold styles.
Orientations of planar elements (cleavage plane, bedding plane, fault plane,...) are given as strike/dip, followed by the azimuth direction of the dip (e.g. 025/30 SE for a plane with strike 025°, dipping 30° towards the SE) and orientations of linear elements (striation, intersection lineation,...) are given as plunge/plunge direction (e.g. 30/025 for a line plunging 30° towards 025). In all cases, an azimuth notation is used for strike and plunge direction going from 0° (N), over 180° (S) to 360° (N).
All outcrop measurements are taken from Debacker (2001). Samples (see also table 2) are from Debacker (2001) and Debacker *et al.* (2004b, 2004c, cf. Debacker *et al.*, 2005).

Bedding (S0; measured in outcrop)

40590-630 m:	1. 146/76SW	2. 141/90SW	3. 142/85SW	4. 141/86SW	5. 324/87NE	6. 144/82SW	7. 323/86NE
8. 144/89SW	9. 322/87NE	10. 140/86SW	11. 140/81SW	12. 138/84SW	13. 318/88NE	14. 135/88SW	15. 317/88NE
16. 314/89NE	17. 312/79NE						
40630-673 m:	18. 132/74SW	19. 112/67S	20. 115/55SW	21. 116/57SW	22. 143/83SW	23. 310/88NE	24. 130/58SW
25. 126/53SW	26. 127/72SW	27. 133/75SW	28. 132/79SW	29. 133/62SW	30. 129/74SW	31. 130/71SW	32. 136/85SW
33. 303/81NE	34. 132/84SW	35. 138/54SW	36. 139/61SW	37. 134/69SW	38. 128/81SW	39. 135/83SW	40. 126/78SW
41. 126/74SW	42. 123/76SW	43. 123/67SW	44. 128/65SW				
40673-685 m:	45. 123/66SW	46. 127/71SW	47. 119/62SW	48. 127/71SW	49. 124/73SW	50. 120/76SW	51. 126/54SW
52. 120/56SW	53. 120/50SW	54. 122/41SW	55. 126/38SW	56. 128/70SW	57. 123/67SW	58. 127/56SW	59. 128/50SW
60. 108/44S							
40685-700 m:	61. 092/46S	62. 096/34S	63. 101/45S	64. 105/54S	65. 114/54SW	66. 131/35SW	67. 137/33SW
68. 130/36SW	69. 130/34SW	70. 114/48SW	71. 120/56SW				
40700-725 m:	72. 119/32SW	73. 108/49S	74. 109/42S	75. 103/51S	76. 102/53S	77. 108/63S	78. 104/67S
79. 107/68S	80. 100/66S	81. 103/62S	82. 093/60S	83. 112/57S	84. 114/71SW	85. 114/72SW	86. 120/75SW
87. 120/76SW	88. 123/79SW	89. 121/63SW	90. 122/60SW	91. 121/61SW	92. 116/46SW	93. 116/49SW	94. 093/49S
95. 106/56S	96. 112/61S	97. 108/55S					
40725-745 m:	98. 306/89NE	99. 125/88SW	100. 123/81SW	101. 130/88SW	102. 127/78SW	103. 126/81SW	104. 125/77SW
105. 130/82SW	106. 122/84SW	107. 123/76SW	108. 122/76SW				
40825-840 m:	109. 046/26SE	110. 080/30S	111. 085/28S	112. 117/62SW	113. 098/54S	114. 106/62S	115. 103/65S
116. 106/53S	117. 105/73S						
40890-910 m:	118. 131/63SW	119. 126/76SW	120. 128/70SW	121. 122/78SW	122. 119/76SW	123. 120/71SW	124. 154/28SW
125. 147/31SW	126. 142/34SW	127. 148/34SW	128. 150/31SW	129. 148/30SW	130. 160/36W		
40910-935 m:	131. 126/22SW	132. 120/24SW	133. 124/36SW	134. 126/37SW	135. 126/35SW	136. 143/31SW	137. 138/36SW
138. 137/34SW	139. 146/28SW	140. 115/79SW	141. 115/78SW	142. 112/74S	143. 111/71S	144. 118/75SW	145. 123/72SW
146. 134/60SW	147. 132/64SW	148. 134/60SW	149. 132/56SW	150. 139/54SW	151. 115/62SW	152. 123/62SW	153. 122/60SW
154. 125/62SW	155. 118/60SW	156. 118/62SW	157. 124/60SW	158. 122/64SW	159. 125/54SW	160. 121/60SW	161. 123/50SW
162. 122/56SW	163. 133/47SW	164. 133/45SW					
40935-960 m:	165. 120/66SW	166. 120/59SW	167. 122/59SW	168. 119/56SW	169. 116/57SW	170. 118/54SW	171. 125/70SW
172. 122/54SW	173. 118/69SW	174. 116/49SW	175. 116/49SW				
40960-980 m:	176. 118/34SW	177. 102/49S	178. 104/47S	179. 113/53SW	180. 102/46S	181. 102/46S	182. 109/44S

****

183. 132/42SW	184. 123/48SW	185. 117/56SW	186. 119/49SW	187. 127/53SW			
<u>40980-41000 m:</u>	188. 128/28SW	189. 148/50SW	190. 136/58SW	191. 133/66SW	192. 128/44SW	193. 131/42SW	194. 114/48SW
<u>41040-050 m:</u>	195. 324/76NE	196. 328/76NE	197. 319/82NE	198. 322/76NE	199. 310/88NE		

Note : measurements 156, 157, 158, 169, 195 and 196 occurred on planes containing sedimentary ripples, measurement 181 on a thin volcanic intercalation.

<u>Bedding measured on oriented samples</u>

See sample list in table 2 for detailed location of samples and corresponding bedding measurement.

<u>40590-630 m:</u>	144/82SW	147/80SW	315/90NE				
<u>40630-673 m:</u>	132/73SW						
<u>40725-745 m:</u>	126/77SW						
<u>40745-750 m:</u>	332/55NE	296/82NE					
<u>40750-825 m:</u>	072/45S	332/67NE	000/77E	328/82NE	326/80NE	327/87NE	318/80NE
15. 323/81NE	337/62NE	024/82SE	336/76NE	334/70NE			
<u>40825-840 m</u>:	104/60S						
<u>40840-850 m:</u>	051/43SE	019/50E	070/57S				
<u>40850-890 m:</u>	125/73SW	125/69SW					
<u>40890-910 m</u>:	122/73SW	148/18SW					
<u>40910-935 m:</u>	112/37S	112/75S	133/61SW				
<u>40935-960 m:</u>	115/59SW	113/48SW					
<u>40960-980 m:</u>	108/45S	103/44S	106/45S	106/42S	111/38S	113/40SW	
<u>40980-41000 m</u>:	139/50SW	134/58SW	127/73SW	111/64S			
<u>41000-020 m:</u>	326/74NE	322/75NE	328/70NE	322/71NE	310/58NE		
<u>41020-41040 m:</u>	329/75NE	326/68NE	311/66NE	322/68NE			
<u>41040-41050 m:</u>	322/73NE						

<u>Cleavage (S1)</u>

<u>40590-630 m:</u>	A. 293/46NE	B. 288/49N	C. 310/41NE	D. 303/48NE	E. 304/65NE	F. 300/47NE	G. 288/59N
H. 300/60NE	I. 302/65NE	J. 284/48N	K. 300/59NE	L. 309/69NE	M. 280/60N	N. 294/58NE	O. 288/48N
P. 298/55NE	Q. 300/69NE	R. 302/60NE					
<u>40630-673 m:</u>	S. 287/60N	T. 300/57NE	U. 298/46NE	V. 297/36NE	W. 299/50NE	X. 289/68N	Y. 302/60NE
Z. 297/56NE	A’. 289/57N	B’. 304/66NE	C’. 303/72NE	D’. 281/70N	E’. 308/80NE	F’. 307/66NE	G’. 286/60N
H’. 295/50NE	I’. 312/43NE	J’. 298/66NE	K’. 322/70NE	L.’ 274/51N			
<u>40673-685 m:</u>	M’. 268/53N	N’. 274/60N	O’. 298/68NE	P’. 301/70NE	Q’. 296/76NE	R’. 272/54N	S’. 287/60N
T’. 295/67NE	U’. 285/62N	V’. 307/66NE	W’. 278/60N	X’. 279/56N			
<u>40685-700 m:</u>	Y’. 314/49NE	Z’. 277/37N	A^{2}. 308/64NE	B^{2}. 278/31N	C^{2}. 293/54NE	D^{2}. 286/75N	E^{2}. 282/50N
F^{2}. 295/53NE	G^{2}. 323/67NE	H^{2}. 299/59NE					
<u>40700-725 m:</u>	I^{2}. 286/44N	J^{2}. 277/52N	K^{2}. 290/53N	L^{2}. 270/44N	M^{2}. 285/53N	N^{2}. 285/64N	O^{2}. 286/50N
P^{2}. 270/42N	Q^{2}. 276/40N	R^{2}. 285/47N	S^{2}. 268/59N	T^{2}. 282/51N	U^{2}. 294/76NE	V^{2}. 271/58N	W^{2}. 277/55N
X^{2}. 290/69N	Y^{2}. 279/47N	Z^{2}. 288/50N	A^{3}. 308/40NE	B^{3}. 269/64N			
<u>40725-745 m:</u>	C^{3}. 298/66NE	D^{3}. 293/47NE	E^{3}. 302/74NE	F^{3}. 297/64NE	G^{3}. 298/72NE	H^{3}. 292/61N	I^{3}. 283/70N
<u>40750-825 m:</u>	J^{3}. 331/69NE	K^{3}. 321/54NE	L^{3}. 315/64NE	M^{3}. 316/61NE	N^{3}. 307/69NE	O^{3}. 308/58NE	P^{3}. 306/68NE
Q^{3}. 309/68NE	R^{3}. 317/59NE	S^{3}. 316/66NE	T^{3}. 309/71NE	U^{3}. 304/72NE	V^{3}. 314/74NE	W^{3}. 307/66NE	X^{3}. 306/68NE
Y^{3}. 318/72NE	Z^{3}. 312/72NE	A^{4}. 310/81NE	B^{4}. 321/78NE	C^{4}. 307/77NE	D^{4}. 310/80NE	E^{4}. 308/76NE	F^{4}. 322/72NE
G^{4}. 313/62NE	H^{4}. 300/66NE	I^{4}. 301/75NE	J^{4}. 318/71NE	K^{4}. 315/87NE	L^{4}. 313/76NE	M^{4}. 310/70NE	N^{4}. 285/54N
O^{4}. 306/82NE	P^{4}. 310/72NE	Q^{4}. 305/60NE	R^{4}. 328/61NE	S^{4}. 305/73NE			
<u>40825-840 m:</u>	T^{4}. 310/82NE	U^{4}. 304/68NE	V^{4}. 313/80NE	W^{4}. 306/58NE	X^{4}. 320/72EE	Y^{4}. 299/70NE	Z^{4}. 300/63NE
A^{5}. 302/80NE	B^{5}. 300/84NE	C^{5}. 300/85NE	D^{5}. 300/56NE	E^{5}. 310/80NE	F^{5}. 307/70NE	G^{5}. 320/73NE	H^{5}. 320/70NE
I^{5}. 292/52N	J^{5}. 312/74NE						
<u>40840-850 m:</u>	K^{5}. 285/67N	L^{5}. 283/50N	M^{5}. 310/75NE	N^{5}. 303/79NE	O^{5}. 302/71NE	P^{5}. 291/61N	Q^{5}. 277/60N
R^{5}. 303/59NE	S^{5}. 300/66NE	T^{5}. 290/55N					
<u>40850-865 m:</u>	U^{5}. 290/70N	V^{5}. 308/67NE	W^{5}. 329/66NE	X^{5}. 298/66NE	Y^{5}. 309/63NE	Z^{5}. 299/71NE	A^{6}. 290/60N
B^{6}. 304/82NE							
<u>40865-890 m:</u>	C^{6}. 315/66NE	D^{6}. 314/72NE	E^{6}. 299/70NE	F^{6}. 310/59NE	G^{6}. 318/74NE	H^{6}. 295/60NE	I^{6}. 302/74NE
<u>40890-910 m:</u>	J^{6}. 280/55N	K^{6}. 294/50NE	L^{6}. 302/71NE	M^{6}. 300/64NE	N^{6}. 292/58N	O^{6}. 320/73NE	P^{6}. 295/61NE
Q^{6}. 281/56N	R^{6}. 286/63N	S^{6}. 316/77NE	T^{6}. 310/74NE	U^{6}. 293/61NE	V^{6}. 300/60NE	W^{6}. 290/62N	
<u>40910-935 m:</u>	X^{6}. 303/62NE	Y^{6}. 290/60N	Z^{6}. 298/63NE	A^{7}. 278/61N	B^{7}. 299/64NE	C^{7}. 305/66NE	D^{7}. 301/79NE
E^{7}. 305/62NE	F^{7}. 299/78NE	G^{7}. 300/60NE	H^{7}. 296/60NE	I^{7}. 305/70NE	J^{7}. 292/56N	K^{7}. 296/72NE	L^{7}. 288/61N
M^{7}. 301/59NE	N^{7}. 293/64NE	O^{7}. 281/68N	P^{7}. 303/77NE	Q^{7}. 296/66NE	R^{7}. 285/62N		
<u>40935-960 m:</u>	S^{7}. 298/70NE	T^{7}. 304/70NE	U^{7}. 298/73NE	V^{7}. 308/66NE	W^{7}. 298/82NE	X^{7}. 296/69NE	Y^{7}. 292/76N
Z^{7}. 284/60N							
<u>40960-980 m:</u>	A^{8}. 279/61N	B^{8}. 286/78N	C^{8}. 300/66NE	D^{8}. 296/65NE	E^{8}. 296/69NE	F^{8}. 301/58NE	G^{8}. 288/68N
H^{8}. 286/71N	I^{8}. 272/55N	J^{8}. 298/69NE	K^{8}. 286/54N	L^{8}. 294/66NE	M^{8}. 283/71N	N^{8}. 292/63N	O^{8}. 294/73NE
P^{8}. 280/73N	Q^{8}. 282/73N	R^{8}. 292/63N					
<u>40980-41000 m:</u>	S^{8}. 287/68N	T^{8}. 292/73N	U^{8}. 294/72NE	V^{8}. 303/79NE	W^{8}. 301/71NE	X^{8}. 291/83N	Y^{8}. 298/78NE
Z^{8}. 294/70NE	A^{9}. 298/76NE	B^{9}. 287/79N	C^{9}. 287/67N	D^{9}. 296/72NE	E^{9}. 296/73NE	F^{9}. 295/74NE	G^{9}. 286/69N
<u>41000-020 m:</u>	H^{9}. 284/58N	I^{9}. 300/61NE	J^{9}. 306/65NE	K^{9}. 299/77NE	L^{9}. 306/67NE	M^{9}. 301/78NE	N^{9}. 304/77NE
O^{9}. 296/72NE	P^{9}. 282/64N	Q^{9}. 302/66NE	R^{9}. 308/71NE	S^{9}. 301/61NE	T^{9}. 313/75NE	U^{9}. 304/58NE	V^{9}. 312/74NE
<u>41020-040 m:</u>	W^{9}. 312/75NE	X^{9}. 291/87N	Y^{9}. 303/78NE	Z^{9}. 306/72NE	A^{10}.298/78NE	B^{10}.300/81NE	C^{10}.311/72NE

****

D^{10}.308/76NE	E^{10}.306/79NE	F^{10}.300/67NE	G^{10}.296/74NE	H^{10}.291/72N	I^{10}.298/78NE	J^{10}.304/81NE	K^{10}.302/79NE
L^{10}.310/77NE	M^{10}.304/85NE						
41040-060 m:	N^{10}.311/78NE	O^{10}.307/73NE	P^{10}.310/76NE	Q^{10}.303/74NE	R^{10}.302/81NE	S^{10}.315/76NE	T^{10}.297/74NE
U^{10}.299/78NE	V^{10}.304/82NE	W^{10}.299/79NE	X^{10}.315/72NE	Y^{10}.307/81NE	Z^{10}.296/63NE	A^{11}.315/76NE	B^{11}.301/72NE
C^{11}.300/81NE							
40060-080 m:	D^{11}.306/81NE	E^{11}.295/71NE	F^{11}.300/82NE	G^{11}.303/69NE	H^{11}.299/76NE	I^{11}.300/76NE	J^{11}.305/74NE
K^{11}.306/79NE	L^{11}.304/83NE	M^{11}.295/75NE	N^{11}.307/73NE	O^{11}.292/61N	P^{11}.309/76NE	Q^{11}.313/88NE	R^{11}.302/80NE
S^{11}.293/81NE	T^{11}.293/78NE	U^{11}.302/86NE	V^{11}.301/88NE				
40080-110 m:	W^{11}.304/87NE	X^{11}.296/79NE	Y^{11}.302/80NE	Z^{11}.308/80NE	A^{12}.305/90NE	B^{12}.305/86NE	C^{12}.303/72NE
D^{12}.302/90NE	E^{12}.303/80NE	F^{12}.304/82NE	G^{12}.302/78NE	H^{12}.303/88NE	I^{12}.306/85NE	J^{12}.308/86NE	K^{12}.300/86NE
L^{12}.301/81NE	M^{12}.292/81N	N^{12}.306/90NE	O^{12}.288/75N	P^{12}.303/86NE			

Cleavage/bedding intersection (measured in outcrop)

40590-630 m:	39/315	32/321	36/318	36/318	28/326	38/318	54/328
46/323	43/325	36/317	44/311	30/315	34/319	33/314	46/319
41/315	40/321						
40630-673 m:	20/305	14/291	38/318	25/309	21/300	25/306	22/301
18/304	15/305	31/308	08/316	19/313	26/300	18/301	09/299
15/301							
40673-685 m:	13/302	13/292	26/297	11/301	03/299	22/286	14/293
14/303	08/299	12/299					
40685-40700 m:	09/102	08/107	07/106	02/107	09/289	12/292	14/302
10/298	14/289	05/293	04/300				
40700-725 m:	07/292	04/289	01/289	06/106	01/104	01/104	05/109
02/101	06/280	05/289	21/294	14/297	09/296	03/118	06/294
02/101	01/104	10/122					
40725-745 m:	19/304	16/300	23/302	17/303	11/302	13/301	17/299
11/299							
40890-910 m:	20/287	18/294	18/293				
40910-935 m:	04/301	09/306	14/305	04/116	04/294	03/113	05/301
16/304	21/297	13/294	07/301				
40935-960 m:	05/298	15/292	15/287	14/300	09/294	13/285	
40960-980 m:	04/106	04/116	05/110	00/284	02/287	11/297	13/293
01/117							
40980-41000 m:	11/288	25/301	11/295	04/288			

Quartz-infilled fractures

40590-745 m:	055/52SE	048/60SE	188/79W	183/76W			
40840-850 m:	204/70NW	200/77W	204/70NW	199/74W	210/68NW	209/81NW	200/74W
40890-41000 m:	045/55SE	032/45SE	023/55SE	019/59E	030/51SE	020/75E	021/70E
018/69E	020/68E	024/65SE	028/56SE	022/66E	025/64SE	187/73W	019/89E
018/90E	017/89E	018/90E	191/69W	193/68W	189/70W	193/85W	195/88W
190/70W	188/71W	190/73W					
41000-110 m:	195/66W	188/58W	187/59W	194/60W	194/61W	183/57W	195/61W
194/62W	200/79W	204/54NW	183/62W	194/71W	192/64W	188/63W	

Slip planes

Of the many linear elements encountered along the section, only those are given which are geometrically proven not to be an intersection lineation with the cleavage. Where known, the sense of movement is added (*N*: normal, *R*: reverse, *D*: dextral, *S*: sinistral, or combinations of these in the case of oblique slip).

40619.5m,1.5m:	on S0 14:	67/315	72/315			
40650 m:	on 300/69NE:	66/359 *R*				
40656 m:	on S0 31:	64/265				
40787 m, 5.5 m:	on 322/88NE:	72/328	on 138/86SW:	69/308	on 144/76SW:	67/278
40834.5 m, 4 m:	on 115:	07/280				
40834.5m, 3 m:	on 116:	09/279				
40974 m, 6 m:	on 272/87N:	39/090	on 278/88N:	50/096	on 273/88N:	43/091
40021.5, 1.5 m:	on 150/90SW:	30/150 *D*	on 148/88SW:	29/149 *D*		
40026m, 1.5 m:	on 334/76NE:	27/147 *D*	on 334/83NE:	31/150 *D*		
40025.5 m, 2 m:	on 325/68NE:	49/352	on 330/70NE:	48/354 *N/S*		
40032 m, 2.5 m:	on 139/88SW:	81/307 *N*				
40031.5, 2.5 m:	on 130/89SW:	59/308 *N/D*	on 134/90SW:	67/314 *N/D*		

40619.5 m, 1.5 m: distance along the canal, followed by the height in outcrop.
on 115: measured on bedding plane 115

Kink band

****

A 0.5 to 1 m wide steeply S-dipping contractional kink band occurs at 40.9035 km, with a downthrow towards the south. See also cleavage measurements in zone 40890 – 40910 m for the cleavage orientations to the north (S1 N-side) and south (S1 S-side) of this structure. S1 inside means cleavage measured inside the kink band. A small fault runs along the northern kink band boundary.

S1 N-side:	Ak. 298/69NE	Bk. 288/72N	Ck. 282/44N			
S1 S-side:	Dk. 303/54NE	Ek. 299/67NE				
S1 inside:	Fk. 039/48SE	Gk. 039/38SE	Hk. 072/46S	Ik. 053/55SE	Jk. 030/45SE	
k.b.boundary*:	1k. 094/81S	2k. 090/84S	3k. 080/77S	4k. 064/69SE	5k. 065/72SE	6k. 066/72SE
bending S1*:	Kk. 295/67NE	Lk. 283/29N	Mk. 067/39SE	Nk. 058/45SE		

*: measured on the northern, faulted, kink band boundary, where locally also a small bending of the cleavage can be observed, related to the overall structure

Sedimentary ripples at 40.932 km, 4 m high

20/294	21/289	14/295	27/289	12/294

Samples

TD180	TD181	TD184	TD185	TD186	TD187	TD188	TD189
TD190*	TD191	TD192	TD193	TD194	TD195	TD196	TD197
TD198	TD199	TD240	TD241	TD242	TD243	TD244	TD245
TD246	TD247	TD248	TD249	TD250	TD251	TD252	TD253
TD254	TD255	TD256	TD257	TD258	TD259*	TD260	TD261
TD262	TD263	TD264	TD265	TD266	TD267*	TD268	TD269
TD270	TD271	TD272	TD273*	TD274	TD275*	TD276	TD277
TD278*	TD279	TD182	TD183	TD1001(c)	TD1002(c)	TD1003(c)	TD1004(c)
TD1005	TD1006	TD1006	TD1007	TD1008	TD1009	TD1010	TD1011
TD1012	TD1013	TD1014	TD1015				

* : sample containing crush breccia/protocataclasite
(c): sample, drilled by means of hand drill (cylindrical)

Timothy N. Debacker
September 2001 – September 2004

Table 2 - Samples taken at outcrop northern Asquempont section 2 (BGD115E0912)

Apart from sample number (column 1), position of sample (column 2) and sample orientation (column 3), also the date of sampling (column 4), the number of thin sections made, and the fabric analyses performed (AMS: anisotropy of magnetic susceptibility performed at University of Leuven; ltAMS: low-temperature AMS, performed at 77K at ETH, Zurich; AARM: anisotropy of anhysteretic remanent magnetism, performed at University of Cergy-Pontoise, France; PFG: X-ray-pole figure goniometry, performed by M. Sintubin at University of Leuven) (column 5) and some remarks are given (column 6). The remarks concern the formation name to which the sample belongs, particular structural, lithological or sedimentological observations (e.g. bedding orientation (S0); cleavage orientation (S1)), sometimes the purpose for sampling, or the orientation of the axes of thin sections (a, b, c). Orientations of planar elements (cleavage plane, bedding plane, fault plane,...) are given as strike/dip, followed by the azimuth direction of the dip (e.g. 025/30 SE for a plane with strike 025°, dipping 30° towards the SE) and orientations of linear elements (striation, intersection lineation,...) are given as plunge/plunge direction (e.g. 30/025 for a line plunging 30° towards 025). In all cases, an azimuth notation is used for strike and plunge direction going from 0° (N), over 180° (S) to 360° (N). The *-symbol after an orientation signifies that the measured plane is overturned. The majority of the samples is taken from Debacker (2001), with additional samples of Debacker *et al.* (2004b, 2004c, 2005), taken for magnetic fabric analyses between 2001 and 2005.

Sample	Position	Orientation	Date	Thin sect.	Remarks/purpose
TD180	Northern Asquempont section 2; 3 m S of post 2029; 40.607 km, 2 m high	252/68N	06/09/99		Oisquercq Fm., Asquempont Member; bedding: **147/80SW**
TD181	Northern Asquempont section 2; 6 m S of	144/82SW	06/09/99	2	Oisquercq Fm., Asquempont Member;

****

Sample	Position	Orientation	Date	Thin sect.	Remarks/purpose
	post 2029; 40.604 km, 7 m high				bedding: **144/82SW**
TD182	Northern Asquempont section 2; 4 m N of fourth post N of Asquempont bridge	292/46N	06/09/99		Oisquercq Fm., Asquempont Member; bedding: **/**
TD183	Northern Asquempont section 2; 4 m N fourth post N of Asquempont bridge	108/82S	06/09/99		Oisquercq Fm., Asquempont Member; bedding: **108/82S**
TD184	Northern Asquempont section 2; 41-380.5 m; 40.6195 km, 1.5 m high	315/90NE, 028/69SE*	15/05/00		Oisquercq Fm., Asquempont Member ; striations ; bedding : **315/90NE**
TD185	Northern Asquempont section 2; 41-342.7 m; 40.6573 km, 1 m high	139/69SW, 128/62SW, 155/28SW	15/05/00	PFG	Oisquercq Fm., Asquempont Member; bedding: **132/73SW**
TD186	Northern Asquempont section 2; 41-253 m; 40.747 km, 0.7 m high	301/48NE	24/05/00	PFG	Oisquercq Fm., Asquempont Member ; bedding : **332/55NE (?)**
TD187	Northern Asquempont section 2; 41-251 m; 40.749 km, 1 m high	296/82NE*	24/05/00		Oisquercq Fm., Asquempont Member ; bedding : **296/82NE (?**, vague)
TD188	Northern Asquempont section 2; 41-214 m; 40.786 km, 6.5 m high	312/77NE* 187/ 74W	25/05/00		Oisquercq Fm., Asq. Mem; bedding: ?, vague alignment parallel to cleavage (321/77NE)
TD189	Northern Asquempont section 2; 41-213.5 m; 40.7865 km, 4.2 m high	314/67NE*, 241/60NW	25/05/00		Oisquercq Fm., Asquempont Member ; bedding : /
TD190	Northern Asquempont section 2; 41-213.5 m; 40.7865 km, 4.2 m high, adjacent to TD189	316/76NE*	25/05/00		Oisquercq Fm., Asquempont Member; bedding: /; deformed
TD191	Northern Asquempont section 2; 41-156 m; 40.844 km, 1.5 m high	308/76NE*	31/05/00		Oisquercq Fm., Asquempont Member; bedding: **019/50E (?)**
TD192	Northern Asquempont section 2; 41-151.2 m; 40.8488 km, 1.7 m high	195/90W	31/05/00	PFG	Oisquercq Fm., Asquempont Member; bedding: **070/57S**
TD193	Northern Asquempont section 2; 41-141 m; 40.859 km, 3 m high	326/80NE*, 100/24S	31/05/00		Oisquercq Fm., Asquempont Member; bedding: /
TD194	Northern Asquempont section 2; 41-99 m; 40.901 km, 2.5 m high	122/73SW	06/06/00		Oisquercq Fm., Asquempont Member; bedding: **122/73SW (?)**
TD195	Northern Asquempont section 2; 41-91.5 m; 40.9085 km, 1.2 m high	271/76N, 306/62NE*	06/06/00	PFG 2	Oisquercq Fm., Asquempont Member; bedding: **148/18SW**
TD196	Northern Asquempont section 2; 41-87 m; 40.913 km, 1.5 m high	112/37S	13/06/00	PFG	Oisquercq Fm., Asquempont Member; bedding: **112/37S**
TD197	Northern Asquempont section 2; 41-84.5 m; 40.9155 km, 7m high	205/80W	13/06/00	PFG, **AMS**	Oisquercq Fm., Asquempont Member; bedding: **112/75S**
TD198	Northern Asquempont section 2; 41-79.5 m; 40.9205 km, 5m high	133/61SW	13/06/00		Oisquercq Fm., Asquempont Member; bedding: **133/61SW (?)**
TD199	Northern Asquempont section 2; 41-52 m; 40.948 km, 2m high	115/59S, 295/78NE*	13/06/00	**AMS**	Oisquercq Fm., Asquempont Member; bedding: **115/59SW**
TD240	Northern Asquempont section 2; 41 km-44 m; 40.956 km, 5.5 m high	112/48S, 311/61NE*	14/06/00		Oisquercq Fm., Asquempont Member; bedding: **113/48SW**
TD241	Northern Asquempont section 2; 41 km-34 m; 40.966 km, 5 m high	128/48SW, 305/74NE*	14/06/00		Oisquercq Fm., Asquempont Member; bedding: **108/45S**
TD242	Northern Asquempont section 2; 41 km-30 m; 40.970 km, 1.5 m high	103/44S	14/06/00		Oisquercq Fm., Asquempont Member; bedding: **103/44S**
TD243	Northern Asquempont section 2; 41 km-30 m; 40.970 km, 1.5 m high	122/84SW, 212/89NW	14/06/00		Oisquercq Fm., Asquempont Member; bedding: **106/45S**
TD243’	Northern Asquempont section 2; 41 km-30 m; 40.970 km, 1.5 m high	/	14/06/00	1	Oisquercq Fm., Asquempont Member; volcanic interstratified rock
TD244	Northern Asquempont section 2; 41 km-30 m; 40.970 km, 1.5 m high	121/42SW	14/06/00		Oisquercq Fm., Asq. Mem.; bedding: **106/42S** (?); volcanic rock in lower part of sample
TD245	Northern Asquempont section 2; 41 km-30 m; 40.970km, 1.5 m high	115/63SW, 328/82NE	14/06/00		Oisquercq Fm., Asq. Mem.; bedding: **111/38S**; volcanic rock in upper part of sample
TD246	Northern Asquempont section 2; 41 km-24.5 m; 40.9755 km, 4.7 m high	109/59S, 110/76S	14/06/00		Oisquercq Fm., Asquempont Member; bedding: **113/40S**
TD247	Northern Asquempont section 2; 41 km-26 m; 40.974 km, 6 m high	144/47SW, 305/85NE*	14/06/00		Oisquercq Fm., Asquempont Member; bedding: /
TD248	Northern Asquempont section 2; 41 km-19 m; 40.981 km, 4 m high	137/55SW, 125/44SW	14/06/00	2 (ac,bc) PFG **AMS**	Oisquercq Fm., Asquempont Member; bedding: **139/50SW** a: 00/115; b: 85/215; c: 05/035
TD249	Northern Asquempont section 2; 41 km-19 m; 40.981 km, 6 m high	121/55SW, 307/81NE*	14/06/00		Oisquercq Fm., Asquempont Member; bedding: **134/58SW**
TD250	Northern Asquempont section 2; 41 km-14 m; 40.986 km, 5 m high	127/43SW	14/06/00		Oisquercq Fm., Asquempont Member; bedding: **127/43SW**
TD251	Northern Asquempont section 2; 41 km-1.5	111/64S,	14/06/00		Oisquercq Fm., Asquempont Member;

****

Sample	Position	Orientation	Date	Thin sect.	Remarks/purpose
	m; 40.9985 km, 2 m high	291/81N*			bedding: **111/64S**
TD252	Northern Asquempont section 2; 41.055 km, 5 m high	302/81NE*	15/06/00		Oisquercq Fm., Ripain Member; bedding: /
TD253	Northern Asquempont section 2; 41.101 km, 3 m high	042/77SE, 294/82NE*	16/06/00		Oisquercq Fm., Ripain Member; bedding: /
TD254	Northern Asquempont section 2; 41.092 km, 2.5 m high	128/87SW	16/06/00		Oisquercq Fm., Ripain Member; bedding: /
TD255	Northern Asquempont section 2; 41.0405 km, 4 m high	303/81NE*, 312/75NE*	16/06/00	2	Oisquercq Fm., Ripain Member; bedding: **322/73NE(?)**
TD256	Northern Asquempont section 2; 41.0395 km, 6 m high	308/74NE*	16/06/00	2 (ac,bc) PFG **AMS** ***ltAMS***	Oisquercq Fm., Ripain Member; bedding: **329/75NE(?)** *a: 00/308; b: 74/038; c: 16/218*
TD257	Northern Asquempont section 2; 41.0295 km, 1.5 m high	305/78NE*	16/06/00		Oisquercq Fm., Ripain Member; bedding: /
TD258	Northern Asquempont section 2; 41.0295 km, 1.5 m high, adjacent to TD257	294/68NE*	16/06/00	2	Oisquercq Fm., Ripain Member; bedding: /; vein oriented 313/46NE
TD259	Northern Asquempont section 2; 41-275 m; 40.725 km, 1.8 m high	204/63NW, 307/74NE, 306/65NE*	21/06/00	2	Oisquercq Fm., Asquempont Member; bedding: /; post or pre-cleavage breccia?
TD260	Northern Asquempont section 2; 41-258 m; 40.742 km, 1 m high	310/ 87NE, 040/72SE*	21/06/00	2 **AMS AARM**	Oisquercq Fm., Asquempont Member ; bedding : **126/77SW**
TD261	Northern Asquempont section 2; 41-241 m; 40.759 km, 2.2 m high	106/67S, 116/70SW	21/06/00		Oisquercq Fm., Asquempont Member; bedding: **072/45S**
TD262	Northern Asquempont section 2; 41-220.5 m; 40.7795 km, 1.3 m high	128/35SW, 210/48NW, 326/80NE*	21/06/00	**AMS**	Oisquercq Fm., Asquempont Member; bedding: **326/80NE**
TD263	Northern Asquempont section 2; 41-213 m; 40.787 km, 0.7 m high	184/59W, 181/21W, 312/71NE*	21/06/00		Oisquercq Fm., Asquempont Member; bedding: **327/87NE**
TD264	Northern Asquempont section 2; 41-179 m; 40.821 km, 0.7 m high	229/85NW, 313/63NE*	21/06/00		Oisquercq Fm., Asquempont Member ; bedding : **337/62NE**
TD265	Northern Asquempont section 2; 41-169 m; 40.831 km, 3 m high	299/46NE, 107/57S	21/06/00		Oisquercq Fm., Asquempont Member; bedding: **104/60S**
TD266	Northern Asquempont section 2; 41-159 m; 40.841 km, 2 m high	299/72NE*	21/06/00	2 (ac,bc) **AMS AARM** ***ltAMS***	Oisquercq Fm., Asq. Mem.; bedding orientation changes : **047/48SE to 055/38SE** *a: 00/299 ; b: 72/ 029 ; c :18/209*
TD267	Northern Asquempont section 2; 41-144 m; 40.856 km, 1.7 m high	307/48NE, 189/80W	21/06/00		Oisquercq Fm., Asq. Mem.; bedding: /; deformed; ductile/brittle, post/pre-cleavage?
TD268	Northern Asquempont section 2; 40.769 km, 1.3 m high	199/40W, 135/88SW	06/07/00		Oisquercq Fm., Asquempont Member; bedding: **000/77E**
TD269	Northern Asquempont section 2; 40.765 km, 1.6 m high	296/68NE*	06/07/00	1	Oisquercq Fm., Asquempont Member ; bedding : **332/67NE**
TD270	Northern Asquempont section 2; 40.7777 km, 0.9 m high	127/76SW, 294/66NE*	06/07/00		Oisquercq Fm., Asquempont Member ; bedding : **328/82NE**
TD271	Northern Asquempont section 2; 40.803 km, 1.8 m high	200/40W, 070/50S, 301/69NE*	06/07/00	**AMS**	Oisquercq Fm., Asquempont Member; bedding: **318/80NE**
TD272	Northern Asquempont section 2; 40.8135 km, 1.5 m high	190/76SW 149/31SW	06/07/00	PFG	Oisquercq Fm., Asquempont Member ; bedding orientation changes : **325/79NE, 320/82NE**
TD273	Northern Asquempont section 2; 40.824 km, 1.4 m high	136/38SW, 234/70NW, 325/72NE*	06/07/00		Oisquercq Fm., Asquempont Member; bedding: /; deformed pre- and post-cleavage?
TD274	Northern Asquempont section 2; 40.822 km, 1.4 m high	125/50SW, 318/43NE*	06/07/00	**AMS AARM** ***ltAMS***	Oisquercq Fm.; vague curved alignment along **033/85SE to 014/79E**; slightly deformed
TD275	Northern Asquempont section 2; 40.861 km, 1.7 m high	302/79NE*	06/07/00		Oisquercq Fm., Asq. mem.; bedding: /; breccia, pre- or post-cleavage? seems pre-cleavage
TD276	Northern Asquempont section 2; 40.8725 km, 0.8 m high	125/73SW	06/07/00	PFG	Oisquercq Fm., Asquempont Member; bedding: **125/73SW**
TD277	Northern Asquempont section 2; 40.8857 km, 0.5 m high	125/69SW, 152/10SW	06/07/00		Oisquercq Fm., Asquempont Member; bedding: **125/69SW**
TD278	Northern Asquempont section 2; 41.005 km, 1.8 m high	177/59W, 301/66NE*	06/07/00		Oisquercq Fm., Asq. mem.; bedding: /; deformed, pre- or post-cleavage?; large pyrites occur

****

Sample	Position	Orientation	Date	Thin sect.	Remarks/purpose
TD279	Northern Asquempont section 2; 41.0155 km, 0.4 m high	302/63NE*	06/07/00	PFG **AMS** **AARM**	Oisquercq Fm.; S0: **324/75NE**; S1: 302/63NE
TD1001 (I)	*Cylinder* Northern Asquempont section 2; 9 m S of P2018: 41.0406 km, 3-3.5 m high	TD1001a-TD1001d		**AMS**	Oisquercq Fm., Ripain Mem.
TD1002 (II)	*Cylinder* Northern Asquempont section 2; 21 m N of P2019: 41.03085 km, 1.5-2 m high	TD1002a-TD1002d		**AMS**	Oisquercq Fm., Ripain Mem.
TD1003 (III)	*Cylinder* Northern Asquempont section 2; 0.5 m S of P2021: 40.929 km, 1.5-2 m high	TD1003a-TD1003e		**AMS**	Oisquercq Fm., Asquempont Mem.
TD1004 (IV)	*Cylinder* Northern Asquempont section 2; 13 m N of P2025: 40.7825 km, 0.5 m high	TD1004a-TD1004f		**AMS**	Oisquercq Fm., Asquempont Mem.
TD1005 (TD001)	Northern Asquempont section 2; 9 m S of P2018: 41.0406 km, 4-4.5 m high	322/75NE		**AMS** **AARM** ***ltAMS***	Oisquercq Fm., Ripain Mem. S0: **322/75NE**; S1: 299/76NE
TD1006 (TD002)	Northern Asquempont section 2; 16 m S of P2018: 41.0336 km, 2 m high	305/85NE*		**AMS** **AARM**	Oisquercq Fm., Ripain Mem. S0: **326/68NE**; S1: 294/65NE; a: 00/305 ; b: 85/035 ; c: 15/215
TD1007 (TD003)	Northern Asquempont section 2; 11.5 m N of P2025: 40.781 km, 0.5 m high	324/75NE*		2 (ac,bc) **AMS**	Oisquercq Fm., Asquempont Mem. S0: **336/76NE**; S1: 324/75NE(?), 313/65NE; *a: 00/324 ; b: 75/054 ; c: 15/234*
TD1008 (TD004)	Northern Asquempont section 2; 11 m N of P2025: 40.7805 km, 2 m high	209/57NW 317/69NE*		**AMS**	Oisquercq Fm., Asquempont Mem. S0: **334/70NE**; S1: 317/69NE
TD1009 (I)	Northern Asquempont section 2; 41.018 km, 1.5 m high (bottom outcrop)	311/69NE* (S1)	13/02/04	**AMS**	Oisquercq Fm., Asquempont Mem.. S0: **328/70NE**; S1: 311/69NE. Dextral striations : 37°S on 338/86E
TD1010 (II)	Northern Asquempont section 2; 41.0205 km, 1.5 m high (bottom outcrop)	311/66NE* (S0?)	13/02/04	**AMS** **AARM** ***ltAMS***	Oisquercq Fm., blue grey, Ripain Mem. (?). S0: **311/66NE(?)**; S1: 291/63N Dextral striations : 32°S on 152/89W
TD1011 (III)	Northern Asquempont section 2; 41.0238 km, 1.8 m high	308/74NE* (S1?)	13/02/04	**AMS**	Oisquercq Fm., Ripain Mem. S0: ?; S1: 308/74NE
TD1012 (IV)	Northern Asquempont section 2; 41.0221 km, 1.8 m high	325/68NE* (S0?)	13/02/04	**AMS**	Oisquercq Fm., Ripain Mem. striated surface: 325/68NE (S0?); S0: **322/68NE**; S1: 307/69NE
TD1013 (V)	Northern Asquempont section 2; 41.0198 km, 1.9 - 2 m high	302/66NE* (S1)	13/02/04	**AMS**	Oisquercq Fm., Ripain Mem. S0: ?; S1: 302/66NE; note: strange ellipses present.
TD1014 (VI)	Northern Asquempont section 2; 41.0178 km, 3. 2 m high; 1.5 – 2 E of TD1009	322/71NE* (S0?)	13/02/04	**AMS**	Oisquercq Fm., Ripain Mem. S0: **322/71NE**; S1: 305/73NE
TD1015 (VII)	Northern Asquempont section 2; 41.0153 km, 1. 5 m high	118/82SW; 298/60NE* (~S1)	13/02/04	**AMS**	Oisquercq Fm., Asquempont Mem. S0: **310/58NE**; S1: 291/65N

Timothy N. Debacker
September 2001 – September 2004

Table 3 - Table showing interpreted bedding and cleavage data from outcrop northern Asquempont section 2 (BGD115E0912), taken from Debacker *et al.* (2004b).

Based on the orientation of bedding and cleavage/bedding intersection six zones can be distinguished, three with a gently plunging cleavage/bedding intersection and fold hinge lines (white), and three with a moderately to steeply plunging cleavage/bedding intersection and fold hinge lines (grey). The former reflect zones of type A folds, the latter zones of type B folds. Based on observations throughout the Sennette valley (e.g. Debacker, 2001 and references therein), the limit between both fold types is taken to correspond with a 35° plunge of the cleavage/bedding intersection and fold hinge lines. Note that the two relatively large zones with a moderate to steep intersection lineation have higher cleavage strike values (>300° in this outcrop) than the two large zones with a gently plunging intersection lineation. Orientations of planar elements (cleavage plane, bedding plane,...) are given as strike/dip, followed by the azimuth direction of the dip (e.g. 025/30 SE for a plane with strike 025°, dipping 30° towards the

****

SE) and orientations of linear elements (intersection lineation,...) are given as plunge/plunge direction (e.g. 30/025 for a line plunging 30° towards 025). In all cases, an azimuth notation is used for strike and plunge direction going from 0° (N), over 180° (S) to 360° (N). B-axis: Beta-axis; cw: clockwise cleavage transection; acw: anticlockwise cleavage transection. Except for the last column, numbers of data are written between brackets.

Outcrop interval	Bedding (S0) measured in outcrop	Sample position: distance, height	Sample number	Bedding (S0*) in sample	Mean cleavage (S1)	S0*/S1-intersection	Angle S0*^S1	S1 transection (to S0)	Large zonation based on orientation data
40590 – 40630 m	(17) mean: 140/88SW B-axis: 24/319	40604 m, 7 m	TD181	144/82SW	297/56NE ± 008 (18)	30/319	49°	003°acw	S0: n = 108 B-axis: 24/135 S0*: n = 5 S0 + S0*: n = 113 B-axis: 25/136 S1: n = 87 mean: 292/57N ± 012° transection: 031°acw (S0)
		40607 m, 2 m	TD180	147/80SW		31/321	52°		
		40619.5 m, 1.5 m	TD184	315/90NE		25/315	38°		
40630 – 40673 m	(27) mean: 129/72SW B-axis: 09/132	40657 m, 1 m	TD185	132/73SW	298/59NE ± 011 (20)	15/307	50°	016°acw	
40673 – 40685 m	(16) mean: 123/59SW B-axis: 05/126	/	/	/	287/62N ± 012 (12)	/	/	020°acw	
40685 – 40700 m	(11) mean: 114/42SW	/	/	/	297/53NE ± 015 (10)	/	/	/	
40700 – 40725 m	(26) mean: 111/59S B-axis: 15/120	/	/	/	282/52N ± 010 (20)	/	/	023°acw	
		40725 m, 1.8 m	TD259	Breccia		/	/		
40725 – 40745 m	(11) mean: 125/82SW B-axis: 15/127	40742 m, 1 m	TD260	126/77SW	295/65NE ± 006 (7)	15/302	39°	017°acw	
40745 – 40750 m	/	40747 m, 0.7 m	TD186	332/55NE	/	54/074	/	/	S0*: n = 1
		40749 m, 1 m	TD187	296/82NE	/	03/296	/	/	S0*: n = 1
40750 – 40825 m	/	40759 m, 2.2 m	TD261	072/45S	311/69NE ± 008 (36)	35/116	85°	/	S0: / S0*: n = 12 B-axis: 59/130 S1: n = 36 mean: 311/69NE 311 ± 008° transection: 017°acw (S0*)
		40765 m, 1.6 m	TD269	332/67NE		67/074	20°		
		40769 m, 1.3 m	TD268	000/77E		70/039	47°		
		40777.5 m, 0.9 m	TD270	328/82NE		51/338	21°		
		40779.5 m, 1.3 m	TD262	326/80NE		52/339	18°		
		40780.5 m, 2 m	TD004	334/70NE		69/045	22°		
		40781 m, 0.5 m	TD003	336/76NE		66/010	25°		
		40786 m, 6.5 m	TD188	/		/	/		
		40786.5 m, 4.2 m	TD189	/		/	/		
		40786.5 m, 4.2 m	TD190	Breccia		/	/		
		40787 m, 0.7 m	TD263	327/87NE		41/330	24°		
		40803 m, 1.8 m	TD271	318/80NE		33/324	13°		
		40813.5 m, 1.5 m	TD272	323/81NE		44/333	17°		
		40821 m, 0.7 m	TD264	337/62NE		59/093	25°		
		40822 m, 1.4 m	TD274	024/82SE		70/047	71°		
		40824 m, 1.4 m	TD273	Breccia		/	/		
40825 – 40840 m	(9) (mean: 099/49S) B-axis: 21/118	40831 m, 3 m	TD265	104/60S	307/71NE ± 008 (17)	18/115	55°	001°cw	S0: n = 9, B-axis: 21/118; S1: n = 17, mean: 307/71NE ± 008°; transection: 001°cw (S0)
40840 – 40850 m	/	40841 m, 2 m	TD266	051/43SE	295/64NE ± 010 (10)	37/104	86°	/	S0: /; S0*: n = 3, B-axis: 47/122 S1: n = 18, mean: 299/66NE ± 012° transection: 019°acw (S0*)
		40844 m, 1.5 m	TD191	019/50E		49/094	66°		
		40849 m, 1.7 m	TD192	070/57S		40/102	74°		
40850 – 40890 m	/	40856 m, 1.7 m	TD267	Breccia	303/68NE ± 012 (8)	/	/	/	
		40859 m, 3 m	TD193	/		/	/		
		40861 m, 1.7 m	TD275	Breccia		/	/		
		40872.5 m, 0.8 m	TD276	125/73SW	308/68NE ± 008 (7)	04/126	39°	/	S0: n = 77 B-axis: 12/294 S0*: n = 19 mean: 119/53SW B-axis: 07/124 S0 + S0*: n = 96 B-axis: 10/298 S1: n = 83
		40885.5 m, 0.5 m	TD277	125/69SW		04/126	43°		
40890 – 40910 m	(13) (mean: 134/50S) B-axis: 18/298	40901 m, 2.5 m	TD194	122/73SW	298/63NE ± 012 (14)	05/301	44°	008°cw	
		40908.5 m, 1.2 m	TD195	148/18SW		08/302	79°		
40910 – 40935 m	(34) mean: 125/54SW B-axis: 12/296	40913 m, 1.5 m	TD196	112/37S	296/65NE ± 008 (21)	02/115	78°	006°cw	
		40915.5 m, 7 m	TD197	112/75S		05/113	40°		
		40920.5 m, 5 m	TD198	133/61SW		16/304	56°		
40935 – 40960 m	(11) mean: 119/58SW B-axis: 10/126	40948 m, 2 m	TD199	115/59SW	297/71NE ± 007 (8)	02/116	50°	012°acw	
		40956 m, 5.5 m	TD240	113/48SW		03/116	61°		
		40966 m, 5 m	TD241	108/45S		01/109	69°		
		40970 m, 1.5 m	TD242	103/44S		04/107	70°		

****

Outcrop interval	Bedding (S0) measured in outcrop	Sample position: distance, height	Sample number	Bedding (S0*) in sample	Mean cleavage (S1)	S0*/S1-intersection	Angle S0*^ S1	S1 transection (to S0)	Large zonation based on orientation data
40960 – 40980 m	(12) mean: 114/47SW	40970 m, 1.5 m	TD243	106/45S	289/66N ± 008 (18)	02/108	69°	/	mean: 295/67NE ± 009° transection: 006°cw (S0) transection: 010°acw (S0*) transection: 003°cw (S0 + S0*)
		40970 m, 1.5 m	TD244	106/42S		02/108	72°		
		40970 m, 1.5 m	TD245	111/38S		01/290	76°		
		40974 m, 6 m	TD247	/		/	/		
		40975.5 m, 4.7 m	TD246	113/40SW		02/290	74°		
40980 – 41005 m	(7) mean: 132/48SW	40981 m, 4 m	TD248	139/50SW	294/74NE ± 005 (15)	21/300	61°	/	
		40981 m, 6 m	TD249	134/58SW		21/300	52°		
		40986 m, 5 m	TD250	127/73SW		21/300	35°		
		40998.5 m, 2 m	TD251	111/64S		04/113	42°		
		41005 m, 1.8 m	TD278	Breccia		/	/		
41005 – 41020 m	/	41015.5 m, 0.4 m	TD279	326/74NE	301/68NE ± 008 (15)	66/006	24°	/	S0: n = 9 mean: 323/77NE (5) and: 271/82N (4) B-axis: 78/029 S0*: n = 5 mean: 325/73NE B-axis S0 + S0*: 76/046 S1: n = 87 mean: 302/77NE 302 ± 006° transection: 000° (S0 +S0*), 002°cw (S0)
41020 – 41040 m	/	41029.5 m, 1.5 m	TD257	/	302/77NE ± 006 (17)	/	/	/	
		41029.5 m, 1.5 m	TD258	/		/	/		
		41033.6 m; 2 m	TD002	326/68NE		62/096	25°		
		41039.5 m, 6 m	TD256	329/75NE		75/063	26°		
41040 – 41060 m	(9); mean: 323/ 77NE (5) and 271/82N (4) B-axis: 78/029	41040.5 m, 4 m	TD255	322/73NE	305/76NE ± 006 (16)	71/080	17°	002°cw	
		41040.6 m, 4.3 m	TD001	322/75NE		75/057	16°		
		41055 m, 5 m	TD252	/		/	/		
41060 – 41080 m	/	/	/	/	301/78NE ± 006 (19)	/	/	/	
41080 – 41110 m	/	41092 m, 2.5 m	TD254	/	302/83NE ± 005 (20)	/	/	/	
		41101 m, 3 m	TD253	/		/	/		
Zones with moderately to steeply plunging intersections					Zones with gently plunging intersections				
S0: n = 9, B-axis: 78/029 S0*: n = 21, B-axis: 51/130 S0* + S0: n = 30, B-axis: 63/110 S1: n = 141; mean: 304/73NE ± 009° B-axis: 20/310 Transection: 005°cw (S0) Transection: 017°acw (S0*) Transection: 010°acw (S0 + S0*) S0 + S0* + S1: n = 171, B-axis: 64/090 S0* + S1: n = 162, B-axis: 59/098					S0: n = 194, B-axis: 12/130 S0*: n = 26, B-axis: 15/131 S0* + S0: n = 220, B-axis: 12/130 S1: n = 187, mean: 295/63NE ± 012° B-axis: 35/316 Transection: 019°acw (S0) Transection: 021°acw (S0*) Transection: 019°acw (S0 + S0*) S0 + S0* + S1: n = 407, B-axis: 05/300 S0 + S1: n = 381, B-axis: 06/300				

Timothy N. Debacker
September 2001 – September 2004

Table 4 - Table of mean bedding, cleavage and fracture data from outcrop northern Asquempont section 2 (BGD115E0912), taken from Debacker *et al.* (2004b).

Because of the lack of cleavage/bedding intersections measured in outcrop northern Asquempont section 2 in zones of type B folds, only the lineations constructed as the intersection of bedding determined on oriented samples (S0*) and cleavage measured in outcrop are given for both the type A and type B folds. For more detail concerning this outcrop, the reader is referred to table 3. B-axis: Beta-axis; ACW: anticlockwise cleavage transection. Orientations of planar elements (cleavage plane, bedding plane, fracture plane,...) are given as strike/dip, followed by the azimuth direction of the dip (e.g. 025/30 SE for a plane with strike 025°, dipping 30° towards the SE) and orientations of linear elements (intersection lineation,...) are given as plunge/plunge direction (e.g. 30/025 for a line plunging

****

30° towards 025). In all cases, an azimuth notation is used for strike and plunge direction going from 0° (N), over 180° (S) to 360° (N).

Outcrop and position	Bedding (S0)	Cleavage (S1)	S1/S0 intersection	S0 and S1 merged	S1-transection	Fractures
N. A. S. 2, type A folds (see table 3)	S0, S0*: n = 220 B-axis: 12/130	n = 187 mean: 295/63NE ± 012° B-axis: 35/316	n = 26: mean: 06/299 ± 009°	n = 407 B-axis: 05/300	019° ACW	n = 30 (infilled) 020/78SE ± 012° B-axis: 22/195
N. A. S. 2, type B folds (see table 3)	S0, S0*: n = 30 B-axis: 63/110	n = 141 mean: 304/73NE ± 009° B-axis: 20/310	n = 17: mean: 68/046	n = 171 B-axis: 64/090	010° ACW	n = 21 (infilled) 197/66W ± 008° B-axis: 35/215

Timothy N. Debacker
September 2001 – September 2004

115E0912 - fig. 1

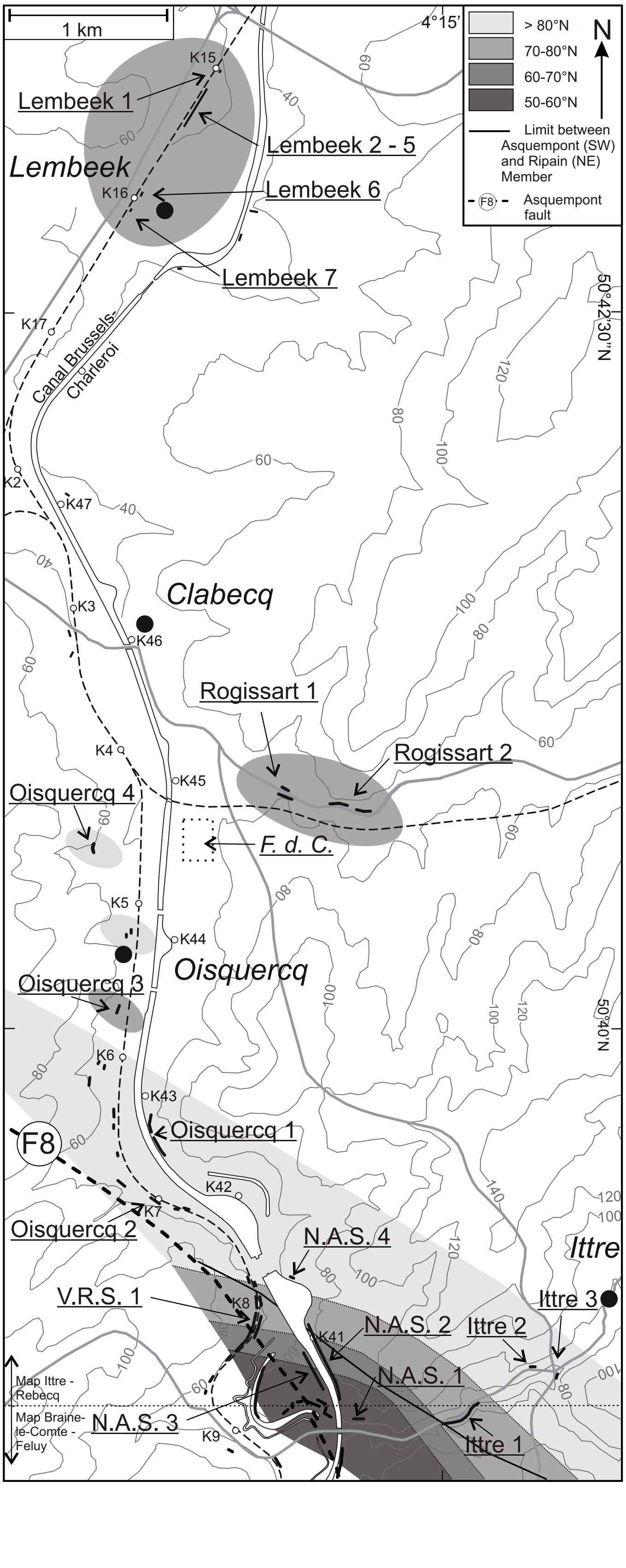

Fig. 1: Simplified map of the study area in the Sennette valley, along the Brussels-Charleroi canal, showing the outcrop positions (in black and labelled; N.A.S.: Northern Asquempont section; V.R.S.: Virginal Railway section; F.d.C.: Forges de Clabecq), the trace of the Asquempont fault (F8; Debacker et al. 2003), the limit between the Asquempont and the Ripain Member, and in grey-shades the mean cleavage dips. Taken from Debacker et al. (2004b).

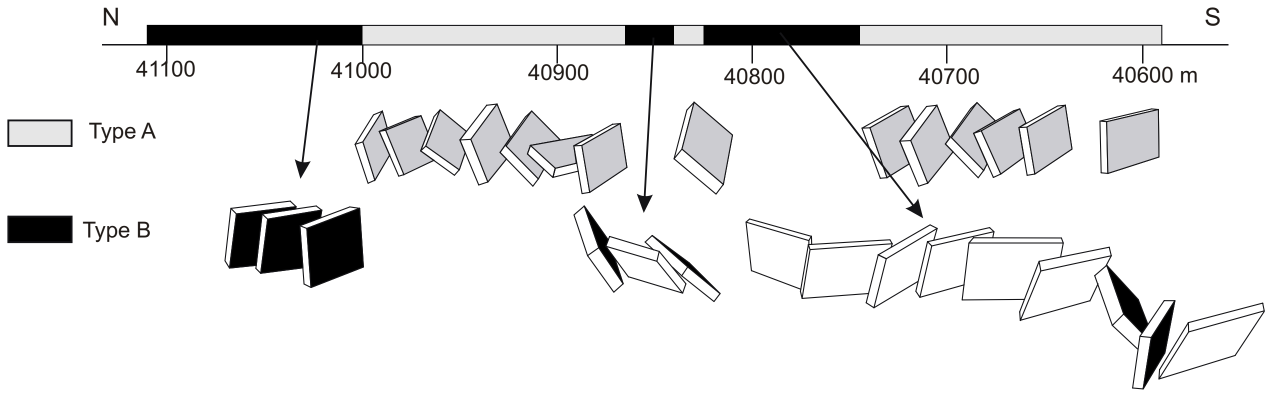

Fig. 2: Schematic representation of the mean bedding orientations along outcrop N.A.S. 2, and the division in fold types, mainly based on the cleavage/bedding relationship (type B folds: steeply plunging fold hinge line and cleavage/bedding intersection; type A folds: gently plunging fold hinge line and cleavage/bedding intersection). Taken from Debacker (2001).

115e0912 - fig.3

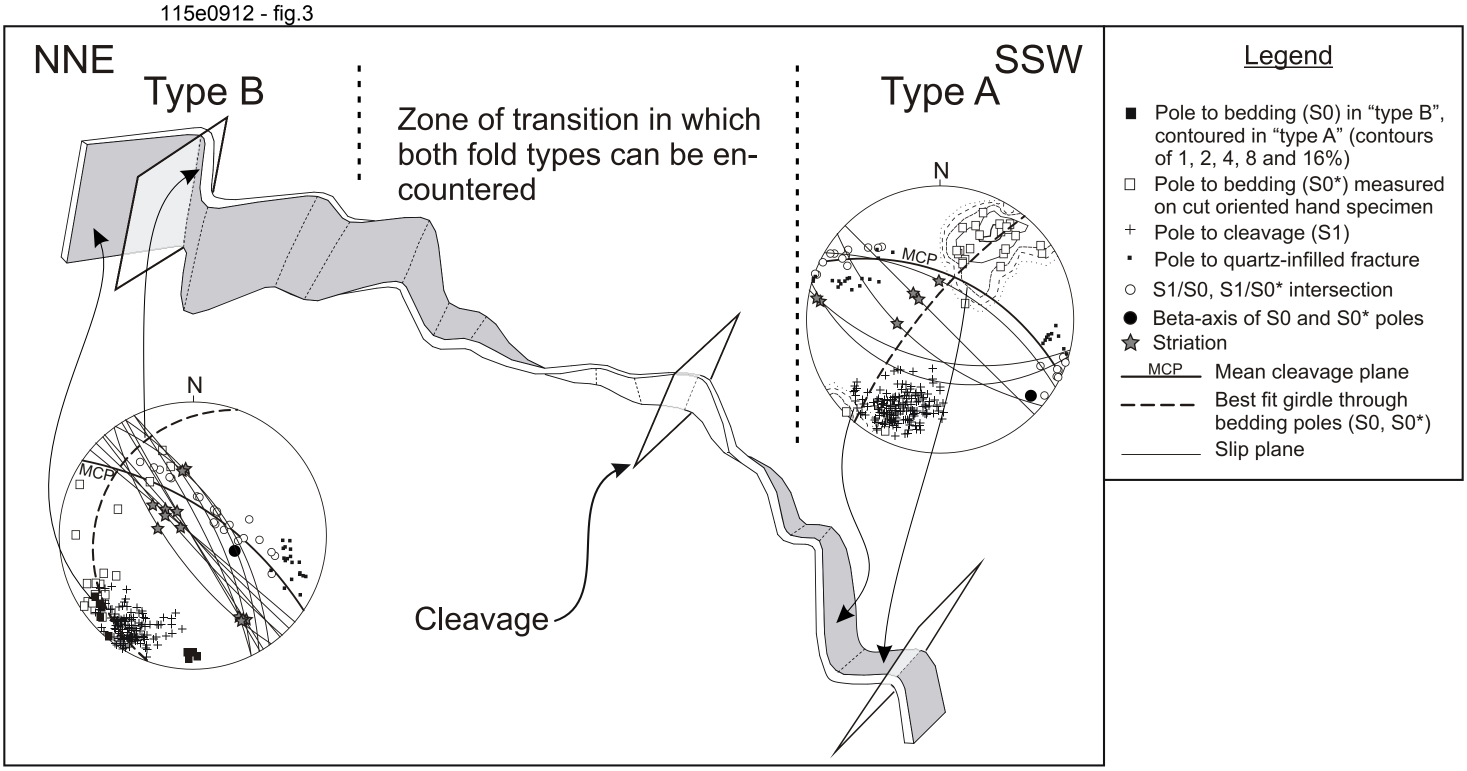

Fig. 3: Schematic representation of bedding geometry within the transition zone between type A folds to the south and type B folds to the north, based on the observations along outcrop N.A.S. 2, with two lower-hemisphere equal-area projections with the structural data related to the type A and type B folds in outcrop N.A.S. 2. Taken from Debacker et al. (2004b).